ARTICLE

Variance reduction adjustment in Monte Carlo TRIPOLI-4®[†] neutron gamma coupled calculations

Odile Petit[*], Yi-Kang Lee and Cheikh M. Diop

*Commissariat à l'Energie Atomique et aux Energies Alternatives,
CEA/DEN/DANS/DM2S/SERMA, 91191 Gif-sur-Yvette Cedex, France*

This paper presents a diagnosis tool for the users of the TRIPOLI-4 Monte Carlo transport code. The aim is to facilitate the adjustment of the variance reduction scheme when dealing with coupled neutron-photon simulations. Up to now, neutron and photon importance functions have been generated independently by TRIPOLI-4 when transport biasing for both particles was necessary, leading to further adjustments by the user after running a first coupled simulation. The idea is here to combine in a fast step the TRIPOLI-4 photon importance map on the one hand, and the photon production data used by the simulation on the other hand, so as to provide at once a better knowledge of important points of neutron phase space with respect to photon tallies. The highest neutron importance mesh cells are then derived and optionally displayed on geometry graphs. The user's intervention consists then in different possible options defining the neutron variance reduction scheme of the TRIPOLI-4 coupled simulation, in the light of the previous diagnosis results. Finally, coupled neutron-photon simulations involving polyethylene and stainless steel slabs are investigated: an example of use of this diagnosis tool is provided and figures of merit related to photon tallies are then compared.

Keywords: Monte Carlo; TRIPOLI-4; variance reduction; coupled neutron-photon simulations; shielding calculations; user diagnosis

1. Introduction

Variance reduction techniques for neutron and photon shielding calculations are commonly used to achieve an adequate convergence of Monte Carlo tallies in an acceptable calculation time. The TRIPOLI-4 [1-3] Monte Carlo transport code provides an efficient biasing scheme with minimal user input data [1,2,4,5] for such simulations. However, when dealing with coupled neutron-photon simulations, variance reduction techniques used for only one of these two particle types do not always reach enough efficiency concerning the photon tallies convergence: thus, TRIPOLI-4 users must sometimes request variance reduction techniques for both neutron and photon transport. Photon and neutron importance maps are then built independently by the code and may lead to further adjustments by the user. The difficulty actually lies in a proper adjustment of the neutron biasing scheme with respect to the photon tallies convergence. The aim of the present diagnosis is to facilitate this adjustment (without delivering a fully automated tool). The main idea is to combine in the initialization step the TRIPOLI-4 photon importance map and the photon production data used by the coupled simulation and read by the code from the nuclear data library.

In the present paper the TRIPOLI-4 biasing scheme is briefly recalled in Section 2 as provided in the version 8 of the code. Section 3 explains then how the diagnosis is built, partly based on the previous biasing scheme, and which output is produced. Section 4 details the user's intervention when adjusting the neutron variance reduction techniques in the light of the diagnosis results. Finally, coupled neutron-photon simulations involving polyethylene and stainless steel slabs are investigated in Section 5 where an example of use of the diagnosis tool is given.

2. Recall of the TRIPOLI-4 biasing scheme

2.1. The INIPOND module

The biasing scheme of TRIPOLI-4 [1] is based on the commonly called Exponential Transform and can be used either for neutrons or for photons or for both, but is independently initialized in that case. It consists in performing transport sampling according to a biased

---

*Corresponding author. Email: odile.petit@cea.fr

[†] TRIPOLI-4® is a registered trademark of CEA.

displacement operator kernel of the following kind:

$$T^*(\mathbf{r}' \to \mathbf{r}, E', \mathbf{\Omega}')\, d\mathbf{r} =$$
$$\Sigma_t^*(\mathbf{r}, E')\exp\left[-\int_0^\rho \Sigma_t^*(\mathbf{r}' + s\,\mathbf{\Omega}', E')\, ds\right] d\rho \tag{1}$$

where $\Sigma_t^*(\mathbf{r}, E')$ is the biased total macroscopic cross-section at point $\mathbf{r}$ and energy E' and ρ is the sampled track length from $\mathbf{r'}$ to $\mathbf{r}$. The different biased macroscopic cross-sections needed for the simulation are derived from the calculation of an importance map in the initialization step of the code (the so-called INIPOND module [1,4,5]) and are defined as follows:

$$\Sigma_t^*(\mathbf{r}, E, \mathbf{\Omega}) = \Sigma_t(\mathbf{r}, E) - [K\,\mathbf{\Omega}\cdot\mathbf{\Omega}_0](\mathbf{r}, E, \mathbf{\Omega}) \tag{2}$$

$$K(\mathbf{r}, E) = \left\|\frac{\vec{\nabla}I(\mathbf{r}, E, \mathbf{\Omega})}{I(\mathbf{r}, E, \mathbf{\Omega})}\right\| \tag{3}$$

$$\mathbf{\Omega}_0(\mathbf{r}, E, \mathbf{\Omega}) = \frac{\vec{\nabla}I(\mathbf{r}, E, \mathbf{\Omega})}{\left\|\vec{\nabla}I(\mathbf{r}, E, \mathbf{\Omega})\right\|} \tag{4}$$

where $\Sigma_t(\mathbf{r}, E)$ is the related natural macroscopic cross-section, $I(\mathbf{r}, E, \mathbf{\Omega})$ is the importance function computed by the code and the unit vector $\mathbf{\Omega}_0(\mathbf{r}, E, \mathbf{\Omega})$ stands for the direction of interest at $(\mathbf{r}, E, \mathbf{\Omega})$ and is computed by taking the gradient of the importance function.

The K values are calculated from the Placzeck-like equation [1,4], based on a few user biasing input data, for each group and each material of the simulation:

$$\Sigma_{st}{}^g I_e{}^g = \frac{\Sigma_t{}^g}{2K^g}\ln\left(\frac{\Sigma_t{}^g + K^g}{\Sigma_t{}^g - K^g}\right)\sum_{g'}\Sigma_s{}^{g\to g'} I_e{}^{g'} \tag{5}$$

$$I_e{}^g = \frac{1}{\beta + 1}\frac{\left(E_{\sup}{}^g\right)^{\beta+1} - \left(E_{\inf}{}^g\right)^{\beta+1}}{E_{\sup}{}^g - E_{\inf}{}^g} \tag{6}$$

where $E_{\sup}{}^g$ and $E_{\inf}{}^g$ are the bounding values for group g, index s stands for scattering and index t for total.

The importance function itself is assumed to be factorized in three parts, spatial, energy and angular, and was detailed in previous references [1,5]. We recall that for the spatial part the user has to define the most important sites of the problem either as discrete attractors or as an analytical attractor surface. The K values are used to compute this spatial part, whereas the biased total macroscopic cross-sections are used to compute the angular part. The energy part is optional and has an exponential form with an appropriate user coefficient for each group of the biasing energy grid.

It should be noted that the β parameter of Eq. (6) has a specific meaning: it behaves as the global strength of the biasing and is chosen by the user typically between 0 and 1. When several discrete attractors are chosen (practically only a few), different β_i parameters can be defined, which enables to attract particles with a suitable intensity towards each attractor.

2.2. Other biasing features

Not all variance reduction techniques available in TRIPOLI-4 are detailed here but most of them can be found in the reference [1]. In addition, a simple but useful feature is mentioned here: for coupled neutron-photon simulations the ratio between photon and neutron populations can be modified, either globally or in given volumes of the geometry, the default value being a ratio of 1. The correction on the statistical weight of photons is done accordingly by the code. This enables for instance to artificially increase the yield of photon production in given materials.

3. The diagnosis tool

3.1. The elements of the diagnosis

3.1.1 The photon importance map

The present diagnosis is partly based on the photon importance map built by TRIPOLI-4 in an initialization step and requested with minimal user input data, in the same way as for a photon-only simulation.

A biasing energy grid has to be defined as well as a three-dimensional mesh encompassing the geometry of the problem. Then, when choosing for instance the discrete attractors option (as recalled at the end of Subsection 2.1), the user has to set an attractor point (or several if needed) at the photon tally position(s). If the requested response function of the tally is a dose rate, an energy part of the importance function may be used in order to enhance the importance of the higher energy groups. The β parameter can be set to 1 for photon deep penetration configurations.

3.1.2 The photon production data

For coupled neutron-photon simulations, additional nuclear data are read by TRIPOLI-4 from the chosen nuclear data library (ENDF/B-VII, JEFF311 or JENDL libraries for example). They consist of photon production data from all possible neutron reactions on the given nuclides of the simulation. They are provided via three possible ways in the nuclear data evaluations [6]: either a photon multiplicity, or a photon production cross-section, or a double differential energy-angle distribution. In all cases a photon multiplicity can be retrieved, possibly through a decay scheme involving several discrete photons, which may be completed by a continuum representation. Photon angular distributions are also used by the simulation in the first two above mentioned cases but are not necessary for the present tool.

To meet the needs of the diagnosis, a photon production matrix **P** is built for each nuclide as the result of the condensation of the photon multiplicities for all possible reactions on a classical threefold spectrum composed of a Maxwell part, a 1/E part and a Watt-Cranberg part. Each element of the matrix can be

written as one of the two following expressions:

$$P(i, j) = \sum_{E_i \in g_i} \sum_{\substack{k \\ E_k \in g_j}} y_k(E_i) f(E_i) \tag{7}$$

$$P(i, j) = \sum_{E_i \in g_i} \sum_{\substack{k \\ E_k \in g_j}} \frac{\sigma_k^\gamma(E_i)}{\sigma(E_i)} f(E_i) \tag{8}$$

where k is either 1 or refers to each photon produced by a decay scheme, $y_k(E)$ and $\sigma_k^\gamma(E)$ are the photon multiplicity and the photon production cross-section for the kth photon respectively, $\sigma(E)$ is the neutron total microscopic cross-section, $f(E)$ is the threefold condensation spectrum, and i and j refer to neutron energy group g_i and photon energy group g_j. Eq.(7) is used when the photon production data of the evaluation are given directly as photon multiplicities (including the double differential energy-angle distribution case), whereas Eq.(8) is used when the photon multiplicities have to be retrieved from the photon production cross-sections provided by the evaluation.

The photon source produced in a given material can then be written as a matrix S_γ whose elements are:

$$S_\gamma(i, j) = \sum_m N_m P_m(i, j) \tag{9}$$

with $\mathbf{P_m}$ the photon production matrix given by Eq.(7) or (8) for nuclide m and N_m the atom density of nuclide m in the given material.

3.2. Establishing the diagnosis

The two previous elements are combined together to derive the neutron importance for the coupled neutron-photon problem:

$$I_n(\mathbf{r}, E_i) = \frac{1}{G} \sum_j \left[S_\gamma(i, j)(\mathbf{r}) \times I_\gamma(\mathbf{r}, E_j) \right] \tag{10}$$

where $I_n(r,E)$ and $I_\gamma(r,E)$ are the neutron and photon importance values at point $\mathbf{r}$ and energy E, actually computed in mesh cells (of the three-dimensional user biasing mesh) and groups (of the user biasing energy grid), $S_\gamma(i,j)$ is given by Eq.(9) for the material present at the center of the current cell, and G is the total number of photon energy groups.

3.3. The provided output

For each neutron energy group, the obtained neutron importance values are sorted by mesh cells from higher to lower importance. The ratio to the maximum importance for each group and the indices of the related cells are then written in the output file of TRIPOLI-4.

For an easier analysis of the diagnosis results, the user has the possibility to request an optional graphical output in addition. It consists in geometrical two-dimensional views where the centers of the most important mesh cells are plotted with a color depending on the ratio of their importance to the maximum importance.

The initialization step of TRIPOLI-4 is sufficient to establish quickly this diagnosis and produce the associated output. The calculation is then stopped and the user's intervention is needed to properly adjust the biasing neutron data of the subsequent full simulation.

4. Possible utilizations of the diagnosis

The previous diagnosis results provide useful information to the user. The adjustment of the neutron TRIPOLI-4 biasing scheme for the current coupled neutron-photon simulation can then be performed by several different ways.

If the diagnosis clearly shows a small number of most important mesh cells, a first possibility is to define discrete neutron attractors (as described at the end of Subsection 2.1) as follows: the attractors are set at the center of those mesh cells and the β_i parameters are set to the related ratios to the maximum importance (for the most relevant biasing group if differences between groups appear, which is not always the case).

A second possibility is to use an analytical form for the neutron attractor (a plane, cylindrical, or spherical surface) if the mesh cells at the highest importance are located on a specific surface (*e.g.*, the exit plane face of a parallelepiped volume).

Finally, as recalled in Subsection 2.2, the increase of the photon production yield for given materials can also be useful if the diagnosis results enhance specific volumes or materials.

5. Application for coupled simulations

To illustrate the diagnosis tool previously detailed, examples of coupled neutron-photon configurations were selected from a series of shielding benchmark experiments [7] and geometry modifications were made for one of them: the purpose was here to magnify different contributing effects of neutron and photon physics. The initial benchmark case [7,8] is a neutron-only problem that involves a neutron source placed in a paraffin collimator, polyethylene and stainless steel slabs arranged with several stainless steel slabs close to the source followed by several polyethylene slabs close to the detector, the whole system being surrounded by air. We modified the slabs arrangement as described in the following and shown in **Figure 1**. The production and transport of photons was also requested in addition when running TRIPOLI-4. The other parameters of the initial benchmark case (point neutron source with a Watt emission spectrum, material compositions, cylindrical detector) were left unchanged. The requested tally is a photon dose rate in the detector.

The geometry modifications consist in placing alternately five stainless steel and five polyethylene

slabs, with a thickness of 5 cm each and separated by a 0.5cm layer of air, between the source and the detector. The ordering of the different slabs from the source side to the detector side is the following: SS, CH_2, SS, CH_2, SS, CH_2, CH_2, SS, CH_2, SS, where SS stands for stainless steel and CH_2 for polyethylene. Figure 1 shows a two-dimensional view of the photon importance map produced by TRIPOLI-4 where the geometry can also be seen. Iso-importance lines are coarsely drawn from the photon importance map computed by the code.
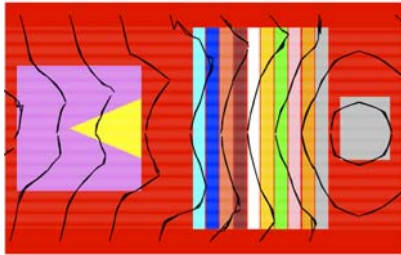
Figure 1. Two-dimensional view with iso-importance lines of the photon importance map produced by TRIPOLI-4. The source is on the left side and the detector on the right side.

The diagnosis finds out that the most important mesh cells, concerning neutron importance, are those located in the five stainless steel slabs. **Figure 2** shows an example of optional graphical output of the diagnosis where red points are displayed at the centers of the most important mesh cells. These results are similar for all neutron groups.
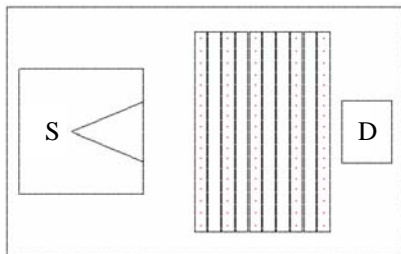

Figure 2. Two-dimensional view of the most important mesh cells, concerning neutron importance. Red points show the centers of most important mesh cells of the neutron biasing mesh.

These results can be understood as follows. The photons produced in the stainless steel slabs are mainly emitted by inelastic neutron scattering reactions and have high energies (7 to 9 MeV). They are therefore responsible for the main part of the photon dose rate, whereas photons produced in polyethylene by capture reactions on hydrogen have lower energies (2.2 MeV) and contribute less to the photon dose rate.

In the light of the previous results, the increase of the photon production yield in stainless steel volumes appears to be relevant. For validation purpose, we compare the efficiency of the variance reduction technique for this choice and for other possible options.

The first option is the analog simulation (no variance reduction technique, neither for photons nor for neutrons, except for the default use of the Russian roulette). The

figure of merit achieved with this option will be the reference for all efficiency calculations.

For the second option we define a variance reduction scheme only for photons, which corresponds to the photon importance map displayed in Figure 1. In this case a discrete attractor is placed at the center of the detector (with a β parameter equal to 1), and an energy part of the photon importance is used so as to enhance the highest energy group (above 1 MeV).

The third option consists in defining a neutron biasing scheme in the same way as for the second option. The β parameter is also set to 1 but this time no energy part is used for the neutron importance.

For the fourth option the previous neutron and photon biasing schemes of options 2 and 3 are used together.

The fifth option is the same as the fourth one but with a lower β parameter of 0.2 for the neutron importance.

Finally, the sixth option consists in using the same photon biasing scheme as for the second option, combined with an increase of the photon production yield of a factor 10 in all stainless steel volumes. This last choice corresponds to the straight use of the diagnosis results.

The results are presented in **Table 1** in terms of figures of merit and efficiencies, regarding the photon dose rate tally in the detector. We recall that the figure of merit is defined by the inverse of the product of the variance of the requested tally and the simulation time. Efficiencies are then derived by normalizing by the figure of merit achieved with option 1.

Table 1. Comparison of figures of merit and efficiencies for different choices of photon and/or neutron biasing schemes (BS) detailed previously. The choice in agreement with the diagnostic results is the sixth.

BS option	Figure of merit	Efficiency
1	2.77	1
2	5.13	1.85
3	6.56	2.37
4	2.37	0.85
5	2.63	0.95
6	22.5	8.12

Option 6 leads to a gain of a factor 8 for the efficiency, which is far better than for the other options. It should be noted that options 4 and 5 apply a neutron biasing scheme that does not take into account the coupled neutron-photon issue: as a result, they lead to worse efficiencies than the analog simulation for the current configuration. The third option (using a neutron biasing scheme only) may sometimes be satisfying for shielding configurations where the contributing photons mainly originate from neutron collisions close to the detector. However, in the present configuration the improvement is not significant and option 6 shows a better efficiency.

Figures 3 and **4** illustrate the sampling of photon collision sites during shorter simulations with options 1 and 6. The two-dimensional views are done in a

different direction as compared to Figures 1 and 2, but there is no impact due to this difference.
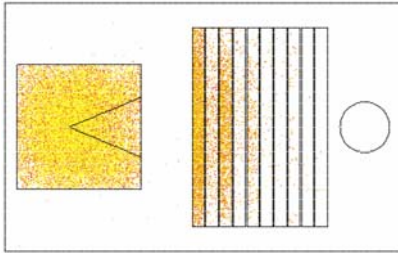

Figure 3.   Two-dimensional view of photon collision sites with option 1. Energies higher than 1 MeV (red points), from 100 keV to 1 MeV (orange points) and lower than 100 keV (yellow points) are differentiated.
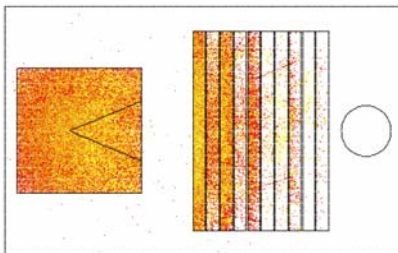

Figure 4.   Two-dimensional view of photon collision sites with option 6. The color meaning is the same as for Figure 3.

These two figures clearly illustrate a qualitative difference in producing and transporting photons, leading to different efficiencies when calculating the photon dose rate.

6. Conclusion

In this paper a diagnosis tool was presented in the frame of coupled neutron-photon Monte Carlo simulations with the TRIPOLI-4 code. Details on the set-up of this diagnosis tool were given and applications were discussed. An example taken from a shielding benchmark was used to illustrate a comparison of the efficiency for the biasing scheme suggested by the diagnostic results and for other different choices. This successfully validated the results of the diagnosis. The application to other configurations including more realistic facilities could be investigated in a future work.

An important remark is finally due: this tool provides a useful help to the user when adjusting the biasing scheme, but is not yet an automatic tool.

References

[1] E. Brun, E. Dumonteil, F.X. Hugot, N. Huot, C. Jouanne, Y.K. Lee, F. Malvagi, A. Mazzolo, O. Petit, J.C. Trama and A. Zoia, Overview of the TRIPOLI-4 version 7 Continuous-Energy Monte Carlo Transport Code, *Proc. ICAPP-2011*, May 2-5, 2011, Nice, France, (2011).

[2] O. Petit, F.X. Hugot, Y.K. Lee and C. Jouanne, *TRIPOLI-4 Version 4 User Guide*, CEA-R-6169, Commissariat à l'Energie Atomique (CEA), France, (2008).

[3] TRIPOLI-4 Monte Carlo Transport Code, http://www.nea.fr/abs/html/nea-1716.html, (2004).

[4] J.P. Both, J.C. Nimal and T. Vergnault, Automated importance generation and biasing techniques for Monte-Carlo shielding techniques by the TRIPOLI-4 code, *Progr. Nucl. Energy* 24 (1990), pp. 273-281.

[5] O. Petit and C.M. Diop, TRIPOLI-4: the automatic variance reduction scheme, *Trans. of the ANS.* 97 (2007), p. 520.

[6] Cross Section Evaluation Working Group, ENDF-102 Data Formats and Procedures for the Evaluated Nuclear Data File ENDF-6, BNL-NCS-44945, National Nuclear Data Center, Brookhaven National Laboratory, (1990).

[7] K. Ueki, A. Ohashi, N. Nariyama, T. Fujita, K. Hattori and Y. Anayama, Systematic evaluation of neutron shielding effect for materials, *Nucl. Sci. Eng.* 124 (1996), pp. 455-464.

[8] C. Solomon, A. Sood and R. Mosteller, *A Polyethylene and Stainless Steel Composite Deep Shield Benchmark of MCNP*, LA-UR-06-2349, Los Alamos National Laboratory, USA, (2006).